Parallel laser micromachining based on diffractive optical elements with dispersion compensated femtosecond pulses

S. Torres-Peiró,[1,2] J. González-Ausejo,[1,2] O. Mendoza-Yero,[1,2] G. Mínguez-Vega,[1,2,*] P. Andrés,[3] and J. Lancis[1,2]

[1]*INIT - Institut de Noves Tecnologies de la Imatge, Universitat Jaume I, Castelló, Spain*
[2]*GROC•UJI - Grup de Recerca d'Òptica, Dept. de Física, Universitat Jaume I, Castelló, Spain*
[3]*Department d'Òptica, Universitat de València, Burjassot (València), Spain*
[*]*gminguez@uji.es*

Abstract: We experimentally demonstrate multi-beam high spatial resolution laser micromachining with femtosecond pulses. The effects of chromatic aberrations as well as pulse stretching on the material processed due to diffraction were significantly mitigated by using a suited dispersion compensated module (DCM). This permits to increase the area of processing in a factor 3 in comparison with a conventional setup. Specifically, 52 blind holes have been drilled simultaneously onto a stainless steel sample with a 30 fs laser pulse in a parallel processing configuration.

OCIS codes: (260.1960) Diffraction theory; (320.2250) Femtosecond phenomena; (220.4000) Microstructure fabrication; (350.3850) Materials processing.

References and links

1. J. Cheng, C.- Liu, S. Shang, D. Liu, W. Perrie, G. Dearden, and K. Watkins, "A review of ultrafast laser materials micromachining," Opt. Laser Technol. **46**, 88–102 (2013).
2. R. Stoian, A. Rosenfeld, D. Ashkenasi, I. V. Hertel, N. M. Bulgakova, and E. E. B. Campbell, "Surface charging and impulsive ion ejection during ultrashort pulsed laser ablation," Phys. Rev. Lett. **88**(9), 097603 (2002).
3. N. M. Bulgakova, R. Stoian, A. Rosenfeld, I. V. Hertel, W. Marine, and E. E. B. Campbell, "A general continuum approach to describe fast electronic transport in pulsed laser irradiated materials: The problem of Coulomb explosion," Appl. Phys., A Mater. Sci. Process. **81**(2), 345–356 (2005).
4. J. Kato, N. Takeyasu, Y. Adachi, H. Sun, and S. Kawata, "Multiple-spot parallel processing for laser micronanofabrication," Appl. Phys. Lett. **86**(4), 044102 (2005).
5. S. Matsuo, S. Juodkazis, and H. Misawa, "Multiple-spot parallel processing for laser micronanofabrication," Appl. Phys., A. **80**, 683–685 (2004).
6. P. S. Salter and M. J. Booth, "Addressable microlens array for parallel laser microfabrication," Opt. Lett. **36**(12), 2302–2304 (2011).
7. D. Kim and P. T. C. So, "High-throughput three-dimensional lithographic microfabrication," Opt. Lett. **35**(10), 1602–1604 (2010).
8. D. N. Vitek, D. E. Adams, A. Johnson, P. S. Tsai, S. Backus, C. G. Durfee, D. Kleinfeld, and J. A. Squier, "Temporally focused femtosecond laser pulses for low numerical aperture micromachining through optically transparent materials," Opt. Express **18**(17), 18086–18094 (2010).
9. S. Shoji and S. Kawata, "Photofabrication of three-dimensional photonic crystals by multibeam laser interference into a photopolymerizable resin," Appl. Phys. Lett. **76**(19), 2668–2670 (2000).
10. T. Kondo, S. Matsuo, S. Juodkazis, and H. Misawa, "Femtosecond laser interference technique with diffractive beam splitter for fabrication of three-dimensional photonic crystals," Appl. Phys. Lett. **79**(6), 725–727 (2001).
11. T. Kondo, S. Matsuo, S. Juodkazis, V. Mizeikis, and H. Misawa, "Multiphoton fabrication of periodic structures by multibeam interference of femtosecond pulses," Appl. Phys. Lett. **82**(17), 2758–2760 (2003).
12. Y. Kuroiwa, N. Takeshima, Y. Narita, S. Tanaka, and K. Hirao, "Arbitrary micropatterning method in femtosecond laser microprocessing using diffractive optical elements," Opt. Express **12**(9), 1908–1915 (2004).
13. Y. Hayasaki, T. Sugimoto, A. Takita, and N. Nishida, "Variable holographic femtosecond laser processing by use of a spatial light modulator," Appl. Phys. Lett. **87**(3), 031101 (2005).
14. S. Hasegawa and Y. Hayasaki, "Adaptive optimization of a hologram in holographic femtosecond laser processing system," Opt. Lett. **34**(1), 22–24 (2009).
15. Z. Kuang, W. Perrie, J. Leach, M. Sharp, S. P. Edwardson, M. Padgett, G. Dearden, and K. G. Watkins, "High throughput diffractive multi-beam femtosecond laser processing using a spatial light modulator," Appl. Surf. Sci. **255**(5), 2284–2289 (2008).

#198477 - $15.00 USD Received 27 Sep 2013; revised 22 Nov 2013; accepted 27 Nov 2013; published 16 Dec 2013

16. Z. Kuang, D. Liu, W. Perrie, S. Edwardson, M. Sharp, E. Fearon, G. Dearden, and K. Watkins, "Fast parallel diffractive multi-beam femtosecond laser surface micro-structuring," Appl. Surf. Sci. **255**(13-14), 6582–6588 (2009).
17. A. Jesacher and M. J. Booth, "Parallel direct laser writing in three dimensions with spatially dependent aberration correction," Opt. Express **18**(20), 21090–21099 (2010).
18. J. Cugat, A. Ruiz de la Cruz, R. Solé, A. Ferrer, J. J. Carvajal, X. Mateos, J. Massons, J. Solís, G. Lifante, F. Díaz, and M. Aguilgó, "Femtosecond-Laser Microstructuring of Ribs on Active (Yb,Nb): RTP/RTP Planar Waveguides," J. Lightwave Technol. **31**(3), 385–390 (2013).
19. J. Amako, K. Nagasaka, and N. Kazuhiro, "Chromatic-distortion compensation in splitting and focusing of femtosecond pulses by use of a pair of diffractive optical elements," Opt. Lett. **27**(11), 969–971 (2002).
20. B. C. Stuart, M. D. Feit, S. Herman, A. M. Rubenchik, B. W. Shore, and M. D. Perry, "Nanosecond-to-femtosecond laser-induced breakdown in dielectrics," Phys. Rev. B Condens. Matter **53**(4), 1749–1761 (1996).
21. L. Englert, M. Wollenhaupt, L. Haag, C. Sarpe-Tudoran, B. Rethfeld, and T. Baumert, "Material processing of dielectrics with temporally asymmetric shaped femtosecond laser pulses on the nanometer scale," Appl. Phys., A Mater. Sci. Process. **92**(4), 749–753 (2008).
22. E. L. Papadopoulou, E. Axente, E. Magoulakis, C. Fotakis, and P. A. Loukakos, "Laser induced forward transfer of metal oxides using femtosecond double pulses," Appl. Surf. Sci. **257**(2), 508–511 (2010).
23. J. R. Vázquez de Aldana, C. Méndez, and L. Roso, "Saturation of ablation channels micro-machined in fused silica with many femtosecond laser pulses," Opt. Express **14**(3), 1329–1338 (2006).
24. J. Lancis, G. Mínguez-Vega, E. Tajahuerce, V. Climent, P. Andrés, and J. Caraquitena, "Chromatic compensation of broadband light diffraction: ABCD-matrix approach," J. Opt. Soc. Am. A **21**(10), 1875–1885 (2004).
25. G. Mínguez-Vega, J. Lancis, J. Caraquitena, V. Torres-Company, and P. Andrés, "High spatiotemporal resolution in multifocal processing with femtosecond laser pulses," Opt. Lett. **31**(17), 2631–2633 (2006).
26. G. Mínguez-Vega, E. Tajahuerce, M. Fernández-Alonso, V. Climent, J. Lancis, J. Caraquitena, and P. Andrés, "Dispersion-compensated beam-splitting of femtosecond light pulses: Wave optics analysis," Opt. Express **15**(2), 278–288 (2007).
27. R. Martínez-Cuenca, O. Mendoza-Yero, B. Alonso, Í. J. Sola, G. Mínguez-Vega, and J. Lancis, "Multibeam second-harmonic generation by spatiotemporal shaping of femtosecond pulses," Opt. Lett. **37**(5), 957–959 (2012).
28. B. Alonso, I. J. Sola, O. Varela, J. Hernández-Toro, C. Méndez, J. San Román, A. Zaïr, and L. Roso, "Spatiotemporal amplitude and phase reconstruction by Fourier-transform of interference spectra of high-complex-beams," J. Opt. Soc. Am. B **27**(5), 933–940 (2010).
29. Ll. Martínez-León, P. Clemente, E. Tajahuerce, G. Mínguez-Vega, O. Mendoza-Yero, M. Fernández-Alonso, J. Lancis, V. Climent, and P. Andrés, "Spatial-chirp compensation in dynamical holograms reconstructed with ultrafast lasers," Appl. Phys. Lett. **94**(1), 011104 (2009).
30. J. Lancis, E. Tajahuerce, P. Andrés, V. Climent, and E. Tepichín, "Single-zone-plate achromatic fresnel-transform setup: Pattern tunability," Opt. Commun. **136**(3-4), 297–305 (1997).

1. Introduction

High precision micro- and nano-structuring of materials with femtosecond laser pulses can only be accomplished under a detailed control of the ablation mechanism. This mechanism can be affected by many factors which include, but are not limited to: material properties i.e., electronic band structures, and laser parameters such as fluence or pulse duration [1]. Hence, the selection of dielectrics, semiconductors or metals for performing ultrafast laser processing strongly determines the nature of the ablation mechanism. For instance, meanwhile laser ablation of dielectrics mainly should be attributed to a multiphoton surface ionization process (Coulomb Explosion), for metals under laser fluence range lower than 1 J/cm^2 the dominate ablation mechanisms seem to be spallation and fragmentation [2, 3]. Under low laser fluence regime, there also occur minimal thermal or mechanical damages in the surrounding of the processed area. This attractive physical phenomenon, together with several well-established techniques for the generation of user-defined irradiance patterns makes femtosecond laser processing a very promising tool for industrial applications. In particular, parallel processing by means of complex irradiance patterns allows overcoming extensive attenuation required for current regenerative or multipass amplifier systems, providing pulse energies in the range of the mJ. Furthermore, it reduces the long fabrication time characteristic of sequentially dot-by-dot scans over a sample. In this context, optical techniques for parallel processing have been used, among other tasks, to generate desired focal patterns with the help of microlens arrays [4–6], get temporal focusing of pulsed beams [7, 8], achieve multibeam interference of femtosecond beams [9–11] or carry out holographic patterning for material micro-structuring by using diffractive optical elements (DOEs) [12–17]. In addition, holographic femtosecond

#198477 - $15.00 USD Received 27 Sep 2013; revised 22 Nov 2013; accepted 27 Nov 2013; published 16 Dec 2013

laser processing assisted by a spatial light modulator (SLM) can be also regarded as a dynamic method for arbitrary irradiance patterning. Note that micro-structured surfaces could be useful i.e., for the fabrication of microfluidic devices [17] or integrated photonics [18].

However, the use of ultrashort pulses for material processing implies to deal with both chromatic aberrations due to the strong dependence of the diffraction phenomenon on the wavelength, and temporal stretching originated by several items i.e., material dispersion or propagation time difference in free space. The former effect reduces the peak intensity and increases the pulse width at the focal point owing to wavelength dispersion. As a matter of fact, it was observed that the eccentricity of holes performed with a DOE at a frequency of 25 lp/mm was increased in a factor of two for a laser of 160 fs [15]. Therefore, the bandwidth of the light source sets an upper limit over the useful processing area to be free from spatial distortion effects. Although several efforts have been conducted to compensate for the spatial distortion, less special care has been paid to keep the temporal width of the incident pulse unchanged over the processing area [12, 17, 19]. Amako et al. demonstrate that a pair of DOEs conduces to a correction of the transversal chromatic aberration, but produces an increase of the pulse duration [19]. Kuroiwa et al. show that the large chromatic dispersion effects induced by DOEs can be reduced when the focalization of the pulse is done with a refractive lens, instead of being included in the DOEs design [12]. Finally, Jesacher et al. propose a way to fabricate 3D structures with high spatial quality by doing machining at different depth of a crystal, but close to the optical axis to avoid chromatic aberration [17].

On the other hand, for non thermal micromachining long pulses can be used (up to the range of about 10 ps depending on the material) [20]. However, optimal energy coupling with the help of suitably shaped temporal pulses gives us the possibility to guide the ablation towards user-defined directions, offering extended flexibility for high-quality material processing. Some experiments have demonstrated the influence of femtosecond shaped pulses in material processing. Just to mention a few cases, asymmetric shaped pulses with third-order dispersion can produce holes smaller than the diffraction limit in dielectrics [21]; with doubled pulses delayed a specific time it is possible to control the size of the transferred spots done in metal oxides [22], and the shape of ablation channels in fused silica can be modified by changing the pulse duration [23].

In this manuscript, we experimentally show that in femtosecond micromachining both chromatic dispersion [24] and pulse stretching can be compensated to a first order with a proper designed DCM. The proposed DCM is made up of a hybrid diffractive–refractive lens triplet [25–27], which allows for wide-field holographic microprocessing under 30 fs pulses with high spatial resolution.

2. Preliminary example

The impact of chromatic aberration and temporal pulse elongation in holographic laser processing can be illustrated by the following example. Let us consider that a diffraction grating of period p_0 is used to generate multifocal spots under pulsed light illumination of central wavelength λ_0. We assume for simplicity that the amplitude of the laser pulse is described by a one-dimensional electric field in the form $U(x,\omega) = U_0 \exp(\frac{-x^2}{4\sigma_x^2}) \exp(\frac{-t^2}{4\sigma_t^2})$ where σ_x and σ_t denote the root-mean-square (rms) width of its spatial and temporal irradiance profiles, respectively. A transform limited pulse with a rms of σ_t has a spectral width σ_λ given by, $\sigma_\lambda = \lambda_0^2 / 4\pi c \sigma_t$. After passing through the diffraction grating the light is focused with a refractive lens of focal length *f*. In the focal plane of the refractive lens a set diffraction orders (denoted by *n*) appears, generating a spatially distributed multifocal pattern. The rms widths of the spatial σ'_x and temporal σ'_t irradiance profiles of the elongated focal spots can be roughly estimated by the expressions [26]

#198477 - $15.00 USD Received 27 Sep 2013; revised 22 Nov 2013; accepted 27 Nov 2013; published 16 Dec 2013

$$\sigma'^{2}_{x} \cong \sigma_0^{2}\left(1+\frac{n^2\lambda_0^2\sigma_x^{2}}{p_0^2c^2\sigma_t^{2}}\right) \quad \text{and} \quad \sigma'^{2}_{t} \cong \sigma_t^{2}\left(1+\frac{n^2\lambda_0^2\sigma_x^{2}}{p_0^2c^2\sigma_t^{2}}\right) \tag{1}$$

respectively, where σ_0 is the rms width of the irradiance profile corresponding to the zero diffraction order which can be calculated by the equation $\sigma_0 = f\,\lambda_0/4\pi\sigma_x$, and c is the speed of light. Note that, the value of σ_0 remains unchanged after removing the diffraction grating. From Eq. (1) is apparent that the higher the diffraction order n, the longer both the spatial elongation in the transversal direction x, and the pulse width.

To have an idea of the spatiotemporal elongation we choose a set of typical parameters $f = 200mm$, $\lambda_0 = 800nm$, $p_0 = 40.5\mu m$ (or 24.7 lp/mm), $\sigma_\lambda = 18.7nm$, and $\sigma_x = 0.75mm$. For the unaffected zero diffraction order ($n = 0$) with $\sigma_0 = 17\mu m$, the pulse duration is kept constant $\sigma'_t = \sigma_t = 9.1fs$ (without taking into account the material dispersion). In contrast, for the first diffraction order ($n = 1$), $\sigma'_x = 94\mu m$, and $\sigma'_t = 50fs$. Hence, the ratios σ'_x/σ_0 and σ'_t/σ_t for the first diffraction order can be roughly estimated in a factor of 5. Such realistic values make the above optical setup unsuitable for applications in holographic parallel microprocessing with broadband pulses.

3. Dispersion compensated module

In order to significantly mitigate the effects of spatial and temporal broadening shown in the previous example, a suited DCM is used. In particular, we choose a hybrid refractive-diffractive DCM that was theoretically introduced in [25]. In Fig. 1 the optical setup is shown.

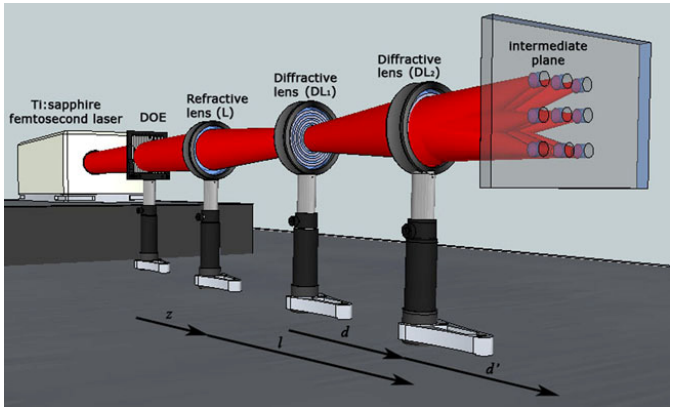

Fig. 1. Schematic of the diffractive-refractive optical system used to improve multifocal micromachining.

Here, it should be mentioned that a diffractive lens (DL) can be regarded as an optical element that focuses light by diffraction, following an inverse dependence with the wavelength of light. The focal lengths of DL_1 and DL_2 for λ_0 are denoted by f_1 and f_2, respectively. Initially, the system acts as a Fourier transformer for the central wavelength, e.g., the field at the output plane is the Fourier transform of the field in the DOE plane for λ_0. Then, we force the design to ensure that the irradiance pattern corresponding to each wavelength coalesces in a single one for all the spectral components of the pulse. In addition, the design also satisfies the condition that every ray impinging onto the DOE must have an identical arrival time at the back focal plane. Although exact compensation is not possible, we impose a first-order correction that leads to the geometrical constraints [25], $l = f$, $d^2 = -f_1 f_2$ and $d' = -d^2/(d + 2f_1)$. These conditions guarantee that in the spatial domain (only for very high spatial frequencies) a residual low spatial elongation is observed, whereas in the time domain some radial group velocity dispersion effects appear [26, 27].

#198477 - $15.00 USD Received 27 Sep 2013; revised 22 Nov 2013; accepted 27 Nov 2013; published 16 Dec 2013

4. Experiment

The experimental setup has mainly three parts, the laser system, the beam delivery block, and the micromachining zone. The light source is given by a mode-locked Ti: sapphire laser (Femtosource, Femtolaser). Following the specification of the manufacturer this laser emits slightly chirped pulses with a full width half maximum of 30 fs ($\sigma_t \approx 13.3fs$). The spectral rms bandwidth measured in our laboratory is approximately $\sigma_\lambda = 18.7nm$ which corresponds to a transform limited pulse of $\sigma_t = 9.1fs$. To reduce the beam size until $\sigma_x = 0.75mm$, an iris is introduced in the beam path. The laser emits pulses with a maximum energy of 0.8 mJ at 1 kHz repetition rate. Before exit the ultrashort pulses pass through a user-adjustable post-compression stage based on fused silica Brewster prisms. Hence, one can introduce negative dispersion to later compensate the positive material dispersion in the beam delivery path.

Initially, the pulse impinges over a DOE (Edmund Optics) designed to provide an array of 8x8 spots in the Fourier plane. This DOE has a design wavelength of 635 nm. The DCM is composed of an achromatic lens L (Thorlabs AC254-200-B), with focal length $f = 200mm$, coupled to the diffractive lens pair, DL_1 and DL_2. The focal of the DLs for λ_0 are $f_1 = -150mm$ and $f_2 = 150mm$, respectively. These DLs were fabricated by a photolithography process, achieving four phase steps and a diffraction efficiency of 80% for λ_0. In particular, they were built over a silicon (Quarglas Substrate) 1mm thickness and 50mm diameter by mask lithography over the positive photoresist (A 3120). The corresponding axial distances in the DCM are $l = 200mm$, $d = 150mm$, and $d' = 150mm$.

In the micromachining zone, the light from the intermediate plane was directed to the laser processing optics, composed of the refractive lens with a focal length of 100mm, and a 20X microscope objective of focal length 10mm, working in a telescope configuration. Between the refractive lens and the microscope objective we placed a shutter to control the number of pulses that arrive to a stainless steel sample. Specifically, this sample was austenitic, Cr-Ni stainless steel type X5CrNi18-10 contained in 3mm thin metal sheet. The sample was mounted on a XYZ translation stage. In these conditions, the sample was irradiated by 500 pulses, forming microstructures onto its surface.

5. Results and discursion

To compare the optical features of the setup shown in Fig. 1 with those of a setup without DCM the DLs pair is removed and the achromatic lens L is displaced. After that, the back focal plane of the lens L was located at the intermediate plane. To determine the energy over the sample with and without the DCM, the irradiance distribution of the focused beam was recorded by using a CCD camera. In order to achieve the same energy for both setups at the zero diffraction order, the input average power was adjusted to 30 mW and 45 mW for the setups with and without DCM, respectively.

The irradiance profiles corresponding to different diffraction orders at the intermediate plane with and without DCM are shown in Fig. 2(a). When the pulse is focused with only the refractive lens (top images), the spatial broadening e.g., for the frequency 11.1 lp/mm is around $\sigma'_x = 52\mu m$. This result is in fairly good agreement with the theoretical value predicted by Eq. (1) which is $\sigma'_x = 45\mu m$. A similar result is obtained for the frequency 24.7 lp/mm (experiment $\sigma'_x = 92\mu m$, and theory $\sigma'_x = 94\mu m$). However, if the DCM is used to focus the light (bottom images), one can observe that focal spots have almost the same shape with a rms width of approximately $\sigma'_x \sim 24\mu m$.

On the other hand, Fig. 2(b) shows the instantaneous intensity for the central point of each diffraction order measured with a recently reported technique [28]. It is based on the spatiotemporal amplitude and phase reconstruction by Fourier transform of the interference spectra of the optical beams (STARFISH). When the pulse is focused with only the refractive lens (top images), the spatial broadening e.g., for the frequency 11.1 lp/mm is around $\sigma'_t = 28.3fs$. This result is in good agreement with the theoretical value predicted by Eq. (1), which is $\sigma'_t = 27.7fs$. A similar result is obtained for the frequency 24.7 lp/mm (experiment $\sigma'_t = 51.2fs$, and theory $\sigma'_t = 52.7fs$). However, if the DCM is used to focus the light (bottom

#198477 - $15.00 USD Received 27 Sep 2013; revised 22 Nov 2013; accepted 27 Nov 2013; published 16 Dec 2013

images), one can observe that the temporal duration is almost the same that the corresponding one at the output of the laser, which is $\sigma'_t \sim 13.5fs$.

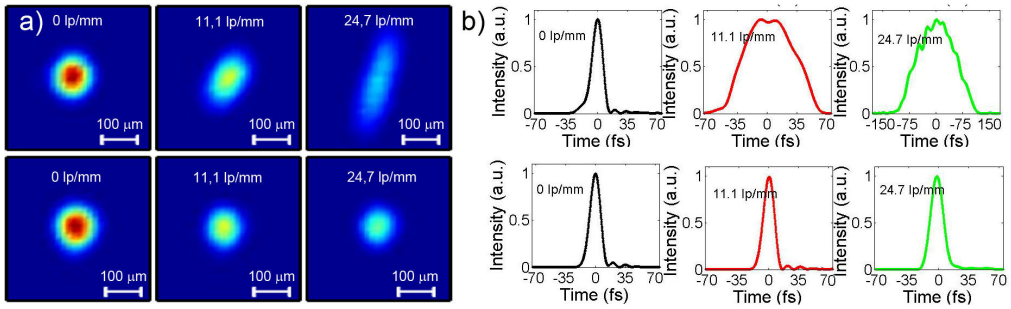

Fig. 2. Measurements in the intermediate focal plane: a) Details of the irradiance profile without DCM (top), and with DCM (bottom). b) Instantaneous intensity for the central point of each diffraction order without DCM (top), and with DCM (bottom).

To see the processed focal spots in a wide spatial field we used an optical microscope. Details of the wide field processed material are shown in Fig. 3(a) and 3(b). In the experiment, 52 blind holes were ablated when the DCM is used (please note that some spots of the DOE were out of the pupil of the microscope objective). This number was reduced to 16 when a conventional setup is employed. Owing to the dispersion effects, in the latter case only focal spots corresponding to lower spatial frequencies had enough fluence to make micromachining in the material surface. In our setup, the highest spatial frequency marked on the metal surface without the DCM was 33 *lp/mm*, while with the DCM we achieved ablation at 50 *lp/mm* what implies an increase of more than 3 times in the ablation area.

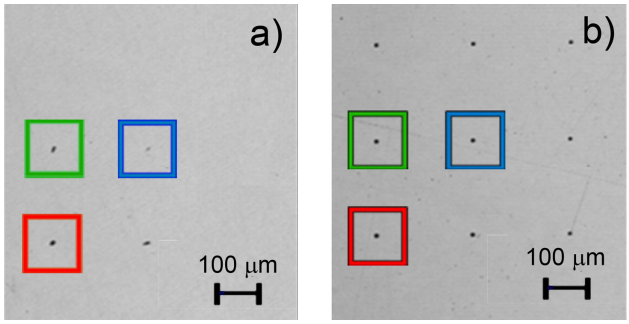

Fig. 3. Details of a region of the surface of the ablated sample observed with an optical microscope (a) with a conventional setup (b) with the DCM.

Spatial features of the ablated material with micrometric resolution were also observed with the help of SEM images, as shown in Fig. 4. In particular, drilled holes obtained for the same spatial frequencies with and without the DCM were compared. From Fig. 4 is it clear that the shape of the processed spots affected by chromatic aberrations departs to a great extent from the ideal circular form. This fact prevents from the use of certain DOEs for micromachining under ultrashort pulsed illumination. However, when the DCM was used the resulted spots retrieved the desired circular shape.

#198477 - $15.00 USD Received 27 Sep 2013; revised 22 Nov 2013; accepted 27 Nov 2013; published 16 Dec 2013

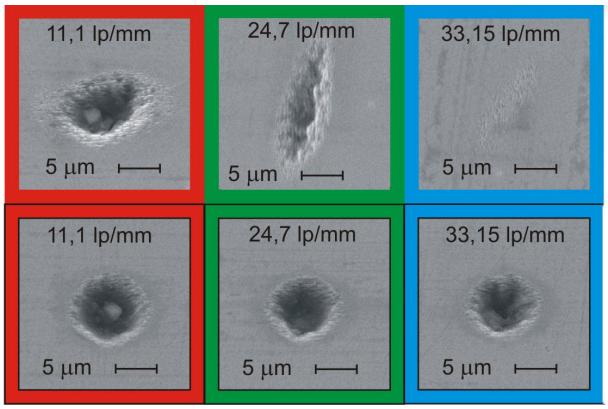

Fig. 4. SEM images of the holes corresponding to different diffraction orders without DCM (top), and with DCM (bottom).

6. Conclusions

We have shown that correction of the chromatic aberration induced by DOEs is mandatory to carry out parallel laser micromachining under ultrashort pulsed illumination. To do that, the integration of a suited diffractive-refractive DCM into the processing line was proposed, and further experimentally validated giving excellent results. The proved ability of the DCM to perform not only spatial but also temporal shaping of ultrashort pulses can be more suited in semiconductors or dielectrics laser microprocessing. In fact, its application to surface nanostructures and/or dielectrics submicro-processing is highly encourage due to the greater sensitivity of these experiments to pulse duration. Note that, the use of spatial light modulator instead of static DOE introduces an additional degree of freedom to the proposed optical setup, allowing for a dynamical processing of the material surface [29]. Meanwhile, in the Fresnel regime the applicability of dispersion compensation modules is a subject of continuing studies [30].

Acknowledgments

This research was funded by the Spanish Ministerio de Ciencia e Innovación through Consolider Programme (SAUUL CSD2007-00013) and project FIS2010-15746. Partial support from the Generalitat Valenciana and the Universitat Jaume I through the projects PROMETEO/2012/021 and P11B2010-26, respectively, is also acknowledged. Authors are also very grateful to the Serveis Centrals d'Intrumentació Científica (SCIC) of the Universitat Jaume I for the use of the femtosecond laser. We are indebted to Professor Jürgen Jahns from the FernUniversität Hagen (Germany) for fabricating the diffractive lenses, and also to professors R. Martínez-Cuenca, B. Alonso, and Í. J. Sola for the help with the temporal characterization of ultrashort pulses.